Non-Homogeneous Media and Ionization Phenomenon Representation in Transient Studies: A TLM Model

Alex B. Tronchoni, Daniel Gazzana, Arturo S. Bretas

***Abstract*—This work proposes a mathematical model to represent ionization phenomenon in non-homogeneous medium based on TLM-2D. Ionization analytical formulation includes dynamic variation of conductive components present in TLM circuit model and residual resistivity retained in ionization region. Non-homogeneous media in TLM-2D method are modeled using reactive and resistive stubs to modify the properties of the medium. A computational implementation based on the TLM-2D algorithm is used to integrate the two developed analytical formulations in a single model. Simulations are presented considering a grounding grid mesh in non-homogeneous media submitted to lightning surges.**

***Keywords*: Grounding, Ionization Phenomenon, Lightning, Non-homogenous media, Transmission Line Modeling.**

I. Introduction

OVER the past decades, numerical methods have been developed and improved for the representation of transient electromagnetic problems associated to the study of atmospheric discharges and its interaction with grounding systems and the surrounding media [1]-[7]. Between several numerical methods options the Transmission Line Modeling method (TLM) stands out. The technique enables the study of the wave propagation phenomena along grounding conductors in materials with non-linear and non-homogeneous properties, with losses, dispersive (frequency dependent) and anisotropic [2].

High currents generated by lightning can trigger the soil ionization phenomenon. This process occurs when electric field E exceeds a certain critical value. The disruption of the soil dielectric caused by this phenomenon should be considered in a trustworthy formulation.

Moreover, conventional methods for soil ionization modeling consider only homogeneous soil conditions, although it is well known that soil is a non-homogeneous media [4], [8]-[18]. Ionization phenomenon modify the properties of the medium and leads to its non-linear behavior, causing reduction in resistivity and consequently increase in conductivity of the medium.

This work was supported in part by CNPq.

Alex B. Tronchoni and Daniel Gazzana are with Universidade Federal do Rio Grande do Sul - UFRGS, Porto Alegre, RS 90035-190, Brazil, (e-mail: alex.tronchoni@ufrgs.br; dgazzana@ece.ufrgs.br).

Arturo S. Bretas is with University of Florida, Gainesville, FL 32611, USA (e-mail: arturo@ece.ufl.edu).

Paper submitted to the International Conference on Power Systems Transients (IPST2019) in Perpignan, France June 17-20, 2019.

In this context, the aim of the paper is to present a numerical conception based on two-dimensional transmission line modeling (TLM-2D) in order to represent the soil ionization phenomenon in a non-homogeneous media focused on grounding system studies submitted to lightning surges.

II. 2D-TLM Formulation

In 1971, Johns e Beurle [1], first introduced the Transmission Line Matrix method (TLM), also known as Transmission Line Modeling method. The solution of Maxwell's equations in this method is performed by analogy between circuit theory and field theory [2]. Based on this equivalence, nonlinearities such as soil ionization, can be solved numerically through models formulated to represent electric conductors, such as grounding systems.

Two-dimensional models are applied for the solution of many problems in engineering, they are simpler to formulate and demands less computational resources than the three-dimensional approach. In a model where one must increase the spatial resolution by a factor of ten, in 2D this would represent an increase in storage by a factor of 100 and for 3D by a factor of 1000.

The concept of the TLM method is based on a discretization of Huygens' theory of light [3], [19]. In a TLM-2D model, waves propagate on a Cartesian coordinate system formed by a mesh of transmission lines interconnected at nodes. Each node communicates with other nodes through four ports and its link lines. Incident pulses at each port from 1 to 4 are scattered at each time step Δt, generating reflected and transmitted pulses from the center of the node [2].

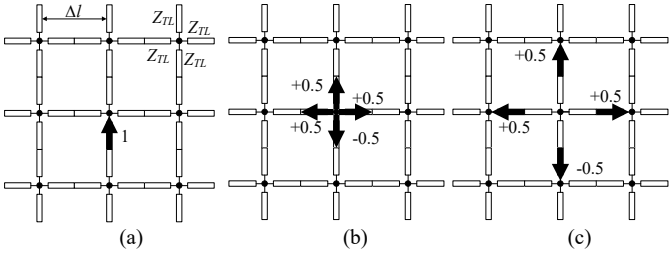

Fig. 1. Transmission line matrix mesh. (a) Pulse incindence at a shunt node. (b) Scattering of incident pulses to the node; (c) Conection of reflected pulses with adjacent nodes.

Fig. 1 presents the basic steps of TLM algorithm. First, a pulse of 1 V magnitude is applied at a node in the TLM mesh, as shown in Fig. 1a. According to the transmission line theory, this pulse is partially reflected and transmitted. Scattering of incident pulses to the node is illustrated in Fig. 1b. In the connection step, Fig. 1c, pulses are transmitted to link lines of adjacent nodes. Thus, reflected pulses at instant k became

incident pulses to neighbor nodes at instant of time $k + 1$.

For $\partial/\partial z = 0$, Maxwell's equations for lossless TM mode are expressed by (1)-(3),

$$\frac{\partial E_z}{\partial y} = -\mu \cdot \frac{\partial H_x}{\partial t} \tag{1}$$

$$\frac{\partial E_z}{\partial x} = \mu \cdot \frac{\partial H_y}{\partial t} \tag{2}$$

$$-\frac{\partial H_x}{\partial y} + \frac{\partial H_y}{\partial x} = \varepsilon \cdot \frac{\partial E_z}{\partial t} \tag{3}$$

where E_z is the electric field along the z-axis (V/m), H_x is the magnetic field along the x-axis (A/m), H_y is the magnetic field along the y-axis (A/m), μ is the permeability of the medium (H/m) and ε is the permittivity of the medium (F/m).

Differentiating (1), (2) and (3) with respect to y, x and t, respectively and combining yields, after simplifying, to the two-dimensional TM wave equation (4):

$$\frac{\partial^2 E_z}{\partial x^2} + \frac{\partial^2 E_z}{\partial y^2} = \mu\varepsilon \cdot \frac{\partial^2 E_z}{\partial t^2} \tag{4}$$

Maxwell's equations may be represented by a matrix of transmission lines. Each TLM node is connected to each other by lumped elements. The equivalent network of a transmission line junction shunt node circuit structure is shown in Fig. 2 [1]-[3].

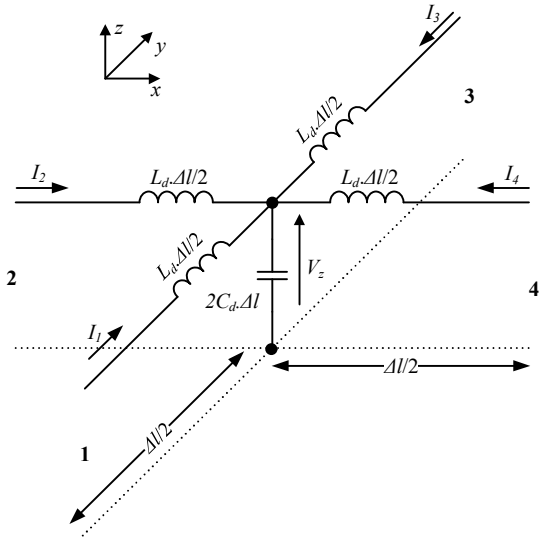

Fig. 2 Equivalent circuit of the TLM shunt node.

Applying Kirchhoff voltage law to the circuit along x-y directions and Kirchhoff current law to x-y plane yields to (5)-(7).

$$\frac{\partial V_z}{\partial x} = -L_d \frac{\partial I_x}{\partial t} \tag{5}$$

$$\frac{\partial V_z}{\partial y} = -L_d \frac{\partial I_y}{\partial t} \tag{6}$$

$$\frac{\partial I_x}{\partial x} + \frac{\partial I_y}{\partial y} = -2C_d \frac{\partial V_z}{\partial t} \tag{7}$$

where V_z is the voltage along the z-axis, I_x is the current along the x-axis, I_y is the current along the y-axis L_d is the inductance per unit length (H/m) and C_d is the capacitance per unit length (F/m).

For a conductor horizontally buried in the soil, its inductance, capacitance and conductance per unit length can be determined according to [12].

Differentiating (5), (6) and (7) with respect to y, x and t, respectively and combining yields, after simplifying, to the shunt transmission line wave equation (8):

$$\frac{\partial^2 V_z}{\partial x^2} + \frac{\partial^2 V_z}{\partial y^2} = 2C_d L_d \frac{\partial^2 V_z}{\partial t^2} \tag{8}$$

Comparing two-dimensional wave equation for voltage in the network (8) and two-dimensional wave equation for electric field in the medium (4) is possible to establish the following equivalences for TM mode (9).

$$E_z = \frac{V_z}{\Delta l} \qquad H_y = -\frac{I_x}{\Delta l} \qquad H_x = \frac{I_y}{\Delta l}$$
$$\mu = L_d \qquad \varepsilon = 2C_d \tag{9}$$

where Δl is the distance between each node.

From these equations, the velocity of propagation u_{TL} (10) and time step Δt (11) on the transmission lines are calculated.

$$u_{TL} = \frac{1}{L_d C_d} = \sqrt{2}\frac{1}{\sqrt{\mu\varepsilon}} \tag{10}$$

$$\Delta t = \frac{\Delta l}{u_{LT}} \tag{11}$$

The transmission line characteristic impedance Z_{TL} is defined by (12).

$$Z_{TL} = \sqrt{\frac{L_d}{C_d}} \tag{12}$$

Solving problems where different materials are present also require modifications in the classical numerical TLM-2D model. Thus, in this work non-homogeneous media and losses are incorporated to the model through appropriate values in the circuit parameters (C, G and L) and adding, whenever necessary, extra inductance (to obtain the desired value of μ) and capacitance (to obtain ε) in the form of stubs [2].

Losses can be incorporated to a medium with conductivity σ by introducing characteristic conductance stub G_s in parallel to the center of the shunt node [2].

Fig. 3 depicts a Thévenin equivalent circuit for the shunt node with a reactive and loss stub Y_s and G_s connected in parallel to the node as two segments of transmission lines.

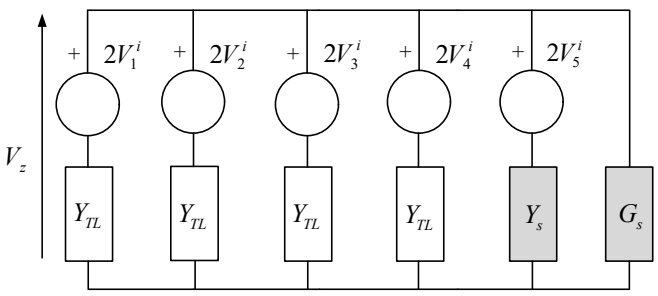

Fig. 3 Thévenin equivalent circuit of the TLM shunt node with a reactive and loss stub Y_s and G_s connected in parallel to the node.

Based on the circuit of Fig. 3, the voltage ${}_kV_z$ on the node can be calculated for each time-step k,

$$ {}_kV_z = \frac{2\cdot\left({}_kV_1^i + {}_kV_2^i + {}_kV_3^i + {}_kV_4^i\right)\cdot Y_{TL} + 2\cdot {}_kV_5^i Y_s}{4\cdot Y_{TL} + Y_s + G_s} \tag{13} $$

where ${}_kV_z$ is the total voltage at the node at each time-step, ${}_kV_1^i$ to ${}_kV_4^i$ are incident voltages pulses at the ports of the shunt node at each time-step (V), ${}_kV_5^i$ is the incident voltage pulse from the reactive stub at each time-step (V), Y_{TL} is the characteristic admittance of the transmission line (Ω^{-1}), Y_s is the characteristic admittance of the reactive stub (Ω^{-1}), G_s is the characteristic admittance of the loss stub (S).

According to [2] the TLM scattering matrix **S** must be modified in order to model different values of permittivity ε_r through the variation of the characteristic admittance Y_s.

III. Ionization Phenomenon

The ionization phenomenon occurs when electric field E exceeds a certain critical value. This critical electric field value E_{cr} is the limit for the beginning of disruption process in the surroundings of the electrode. Discharge channels emerges with much lower resistivity in relation to the medium, facilitating the current dissipation through these paths.

During a transient discharge, soil ionization effect may reduce the grounding system impulsive impedance [8]. Several researches concentrate on the study of this phenomenon with consequent development of representative models, general or not with distinct approaches [4], [9]-[14].

The variable geometry approach [12], [15], [16] can be understood as if the electrode assumed a larger diameter than its original value, as illustrated in Fig. 4. As a consequence, there is a modification in the circuit elements used to model de conductor.

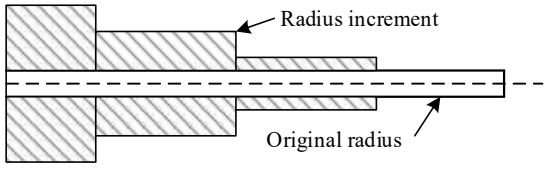

Fig. 4. Electrode radius increment in the ionization region according to Velazquez model.

Methodologies developed by Liew and Darveniza [9], [10] and Sekioka et al [11] focus on a dynamic model to represent the nonlinear variation of the resistivity in the ionization region with the current density.

Mokhtari and Gharehpetian [18] propose an extension of the CIGRE model [20], introducing the effects of arcing in soil resistance considering the energy balance of soil ionization.

Fig. 5a illustrates regions considered in Liew-Darveniva model to represent soil ionization phenomena. Soil disruption is identified by region "b"; the fictitious increment of the electrode radius is given by $r + \Delta r$.

Fig. 5b shows the resistivity profiles model. In region "a" there is a non-ionization region, resistivity remains constant at its initial value ρ_0 until the current density J exceeds the critical value J_{cr}, defined as $J_{cr} = E_{cr} / \rho_0$; ionization starts in region "b", when the current density is greater than the critical value J_{cr} and the resistivity decreases to its initial value.

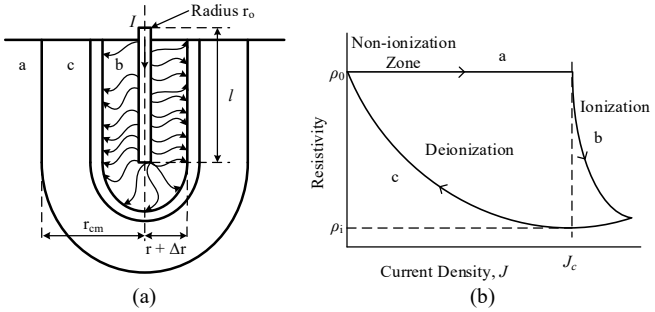

Fig. 5. (a) Regions considered in Liew-Darveniva model; (b) Resistivity profiles in dynamic-impulse resistance model. Adapted from [9].

IV. Analytical Formulation

Based on the concept that the soil ionization produces an increase in the electrode radius, it can be stated that the soil disruption may be partially represented if the increase in the conductance G is considered in the TLM circuit elements

According to the work presented in [17], it is observed the soil retains certain residual resistivity in the ionization region. In compliance with this concept and considering the studies performed by Liu [4], Liew and Darveniza [9], Bellaschi et al. [21], and Oettle [22]; the percentage of residual resistivity in the ionization region for the soils with resistivity ranging from 50 Ω·m to 827 Ω·m can be estimated.

Table I shows some of the mean percentages of residual resistivity in the soil considering the referred experiments.

TABLE I
Mean Values of Residual Soil Resistivity

Soil Resistivity ρ_s (Ω·m)	Experiment	Percentages of Residual Resistivity $\rho_{r\%}$(%)
50	Liew and Darveniza	15.33
157	Bellaschi	6.95
310	Bellaschi	5.5
356	Liu	6.47
579	Liu	6.93
646	Oettle	6.75
827	Liu	20.85

The nonlinear conductance in time $G(t)$ can be estimated by using (14) for a horizontal electrode,

$$ G(t) = \frac{2\cdot\pi\cdot\Delta x}{\rho_s(1-\rho_{r\%})\cdot\left[ln\left(\frac{2\cdot l}{\sqrt{2\cdot h\cdot a}}\right)-1\right]}\cdot\sqrt{1+\frac{I(t)}{I_g}} \tag{14} $$

where G is the conductive component in the TLM model (S), l is the electrode length (m), h is the buried deep (m), a is the electrode radius. I is the lightning current (A), I_g is the lightning current from which the soil ionization initiates (A), ρ_s is the soil resistivity (Ω·m) and $\rho_{r\%}$ is the percentages of residual resistivity (%).

V. Numerical Implementation

Soil ionization can be inserted into the TLM-2D algorithm, as shown in the flowchart of Fig. 6. The electric field E is calculated at all nodes N of the mesh for every instant of time, if the electric field is greater than the critical electric field E_{cr}, equation (14) is used to compute a new value of conductance

G and updated for node N for the next instant of time. In the case of nodes in which the electric field E did not exceed the limit E_{cr}, the values of G remain the same, according to its original values calculate at the initialization of the algorithm.

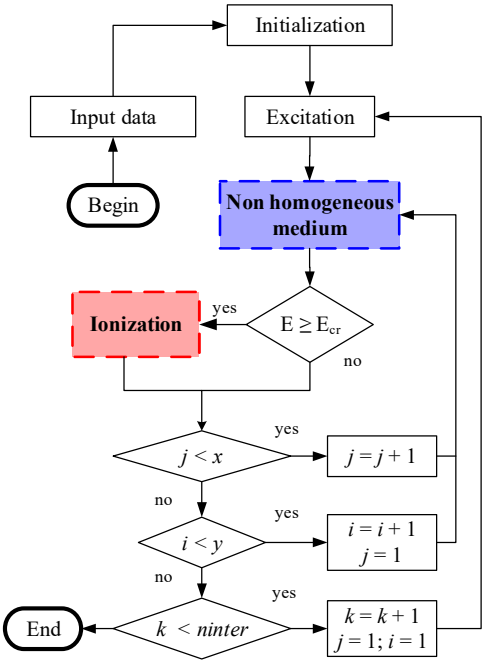

Fig. 6. Flowchart of the TLM-2D algorithm for non-homogeneous medium considering ionization.

VI. Simulation Results

To clarify the proposed technique, a square grounding mesh composed by horizontal conductors buried in soil is considered. It is divided in two identical parts size with different soil properties, characterizing a non-homogeneous media. The soil properties are presented in Table II. Deficit of permittivity is compensated adding capacitive stubs to the model.

TABLE II
Soil Properties in Region 1 and Region 2 of the Mesh

	ε_r	ρ (Ω·m)
Region 1	6	600
Region 2	12	100

The grounding mesh regions and its points of study are illustrated in Fig. 7. It is 20 m x 20 m and 10 x 10 squares of 2 m x 2 m and radius a = 0.0065 m. The conductors were buried at h = 0.5 m depth.

Per unit transmission line parameters are calculated for both sides of the grid according to [12]. For region 1: L_1, C_1, G_1; and for region 2: L_2, C_2, G_2. Thus each side will have different values of Z_{TL},

$$Z_{TL1} = \sqrt{\frac{L_{d1}}{C_{d1}}} \tag{15}$$

$$Z_{TL2} = \sqrt{\frac{L_{d2}}{C_{d2}}} \tag{16}$$

In order to model a space with different properties it is necessary to choose a reference medium, which must have the smallest permittivity value among the other regions. The properties (μ, ε, ρ, and Z_{TL}) of the reference medium are set to the whole space in study, characterizing a homogeneous medium. Thus, non-homogeneities and losses are incorporated to the model in the form of stubs.

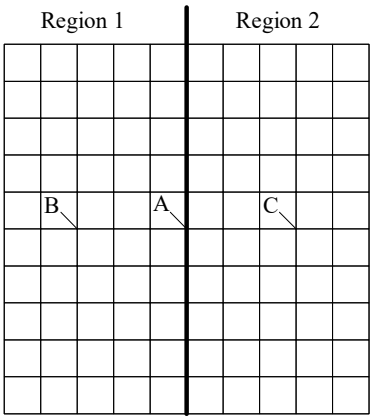

Fig. 7. Grounding grid under simulation and its two regions with different soil properties.

The lightning was simulated by a double exponential wave of 50 kA (1/10) μs shown in Fig. 8 injected at point A of the mesh.

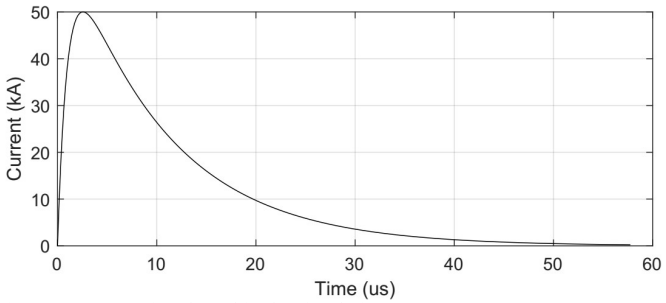

Fig. 8. Current signal used in the simulation.

Fig. 9 illustrates the propagation of the signal injected in the grounding grid in non-homogeneous medium considering soil ionization in the model at instant of time 0.2542 μs when the voltage reaches its peak value in point A.

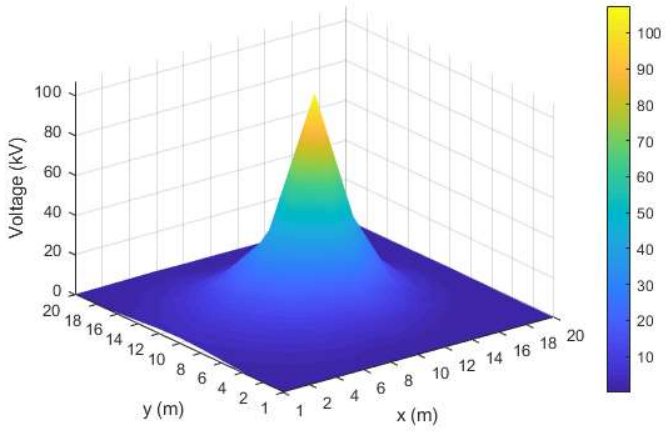

Fig. 9. Wave propagation in the grounding grid in non-homogeneous medium considering soil ionization at instant of time 0.2542 μs.

Fig. 10 shows a schematic top view of the injected current superimposing the grounding grid considering soil ionization at instant of time 1.456 μs.

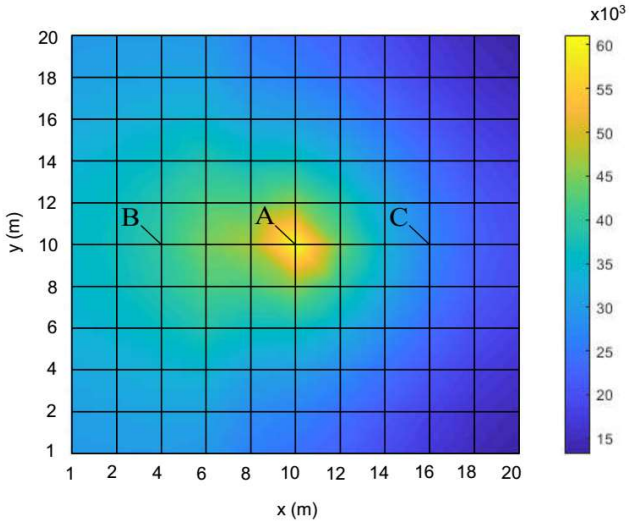

Fig. 10. Injected signal superimposing the grounding grid at instant of time 1.456 µs.

Analyzing Fig. 11, Fig. 12 and Fig. 13, it can be noticed a voltage reduction in points A, B and C. The decrease of potential produced in the electrodes is caused when the soil ionization phenomenon is considered in the model.

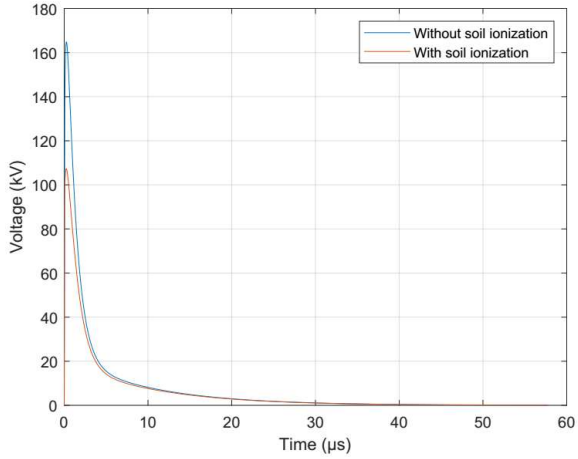

Fig. 11. Voltage at point A with and without considering soil ionization with peak value at instant of time 0.2542 µs.

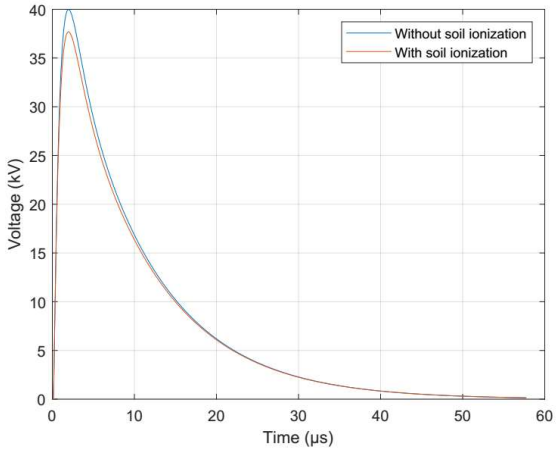

Fig. 12. Voltage at point B with and without considering soil ionization with peak value at instant of time 1.964 µs.

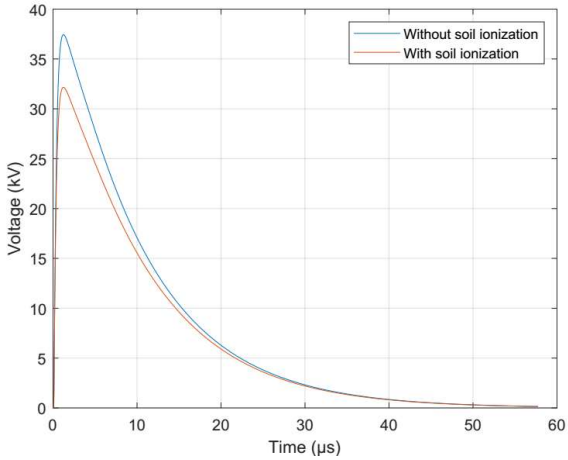

Fig. 13. Voltage at point C with and without considering soil ionization with peak value at instant of time 1.225 µs.

Table III summarizes the simulated results obtained in each point A, B and C of the grounding grid. As can be seen, the potential at these points decreases when soil ionization phenomenon is included in the model. Furthermore, the results highlight the influence non-homogeneous medium also has when is considered simultaneously with ionization.

TABLE III
COMPARISON BETWEEN THE MAXIMUM VOLTAGE PERCENTAGE REDUCTION WITH AND WITHOUT IONIZATION AT POINTS A, B AND C

Point	ε_r	ρ (Ω·m)	V_{max} without ionization (kV)	V_{max} with ionization (kV)	Maximum reduction (%)
A	6	600	164.9	107.4	34.9
B	6	600	40	37.7	5.8
C	12	100	37.4	32.1	14.2

VII. VALIDATION

Several studies in literature assume homogeneous medium in order to represent nonlinearities [8]-[10], [14]. Thus, it is difficult to compare the presented model with state of the art solutions.

Two cases were simulated separately considering a homogeneous medium, $\varepsilon_r = 13$ and $\rho = 200$ Ω·m and $\varepsilon_r = 10$ and $\rho = 500$ Ω·m. The excitation was simulated by a double exponential wave of 50 kA (8/20) µs injected in the center of the mesh. It is 15 m x 15 m and 20 x 20 squares of 0.75 m x 0.75 m. Table IV summarizes simulation results using the proposed methodology (TLM-2D) and the values obtained in [14] (TLM-1D) with and without considering soil ionization. As one can see, results demonstrates good accuracy of the technique.

TABLE IV
COMPARISON BETWEEN THE MAXIMUM VOLTAGE PERCENTAGE REDUCTION WITH AND WITHOUT IONIZATION USING TLM-1D [14] AND TLM-2D.

Model	ε_r	ρ (Ω·m)	V_{max} without ionization (kV)	V_{max} with ionization (kV)	Maximum reduction (%)
TLM-1D [14]	13	200	624.13	543.44	12.93
TLM-2D			643.18	579.86	9.85
TLM-1D [14]	10	530	1651.6	1377.2	16.61
TLM-2D			1686.9	1467.1	13.03

VIII. Conclusions

In this paper, a study based on the TLM-2D for the numerical representation of non-homogeneous medium and ionization was introduced. Basic aspects related to the analytical formulation and numerical implementation of the classical TLM-2D method were also presented.

A brief review about the ionization phenomenon followed by the analytical formulation of how the nonlinear conductance varying in time *G(t)* can be estimated for a horizontal electrode considering the residual resistivity in ionization region. The residual resistivity in the is suitable for soil ranging from 50 Ω·m to 827 Ω·m [4] according to measurements.

The analytical formulation developed to represent ionization phenomena was incorporated into the mathematical model of non-homogeneous media. This formulation was implemented numerically to an integrated model supporting the representation of non-homogeneous media and considering the effect of ionization phenomenon. Simulations performed of the proposed model verified that the obtained results had relevant decrease of the maximum percentage reduction potential values with and without ionization.

It can be observed through the results that the developed methodology can be used for the representation of non-homogeneous media and ionization phenomenon as well.

IX. References

[1] P. B. Johns and R. L. Beurle, "Numerical solution of 2-dimensional scattering problems using a transmission-line matrix," *Proceedings of the Institution of Electrical Engineers*, vol. 118, no. 9, pp. 1203–1208, Sep. 1971.

[2] C. Christopoulos, *The Transmission-Line Modeling Method - TLM*. New York: IEEE Press, 1995.

[3] W. J. R. Hoefer, "The Transmission-Line Matrix Method--Theory and Applications," *IEEE Trans. Microw. Theory Tech.*, vol. 33, no. 10, pp. 882–893, Oct. 1985.

[4] Y. Liu, "Transient response of grounding systems caused by lightning: modelling and experiments," Ph.D. dissertation, Faculty of Science and Technology, Univ. Uppsala, 2004.

[5] S. Fortin, Y. Yang, J. Ma, and F. P. Dawalibi, "Electromagnetic fields of energized conductors in multilayer soils," in *Proc. 2006 4th Asia-Pacific Conference on Environmental Electromagnetics*, pp. 893-899.

[6] L. Grcev, "Computer analysis of transient voltages in large grounding systems," *IEEE Transactions on Power Delivery*, vol. 11, no. 2, pp. 815-823, Apr. 1996.

[7] A. P. Meliopoulos, and A. D. Papalexopoulos, "Frequency dependent characteristics of grounding systems," *IEEE Transactions on Power Delivery*, vol. 2, pp. 1073-1081, Oct. 1987.

[8] A. M. Mousa, "The soil ionization gradient associated with discharge of high currents into concentrated electrodes," *IEEE Transactions on Power Delivery*, vol. 9, no. 3, pp. 1669-1677, Jul. 1994.

[9] A. C. Liew, and M. Darveniza, "Dynamic model of impulse characteristics of concentrated earths," in *Proceedings of the Institution of Electrical Engineers*, vol. 121, no. 2, pp. 123-135, Feb. 1974.

[10] J. Wang, A. C. Liew, and M. Darveniza, "Extension of dynamic model of impulse behavior of concentrated grounds at high currents," *IEEE Transactions on Power Delivery*, vol. 20, no. 3, pp. 2160-2165, Jul. 2005.

[11] S. Sekioka, M.I. Lorentzou, M.P. Philippakou, and J. M. Prousalidis, "Current-dependent grounding resistance model based on energy balance of soil ionization," *IEEE Transactions on Power Delivery*, vol. 21, no. 1, pp. 194-201, Jan. 2006.

[12] R. Velasquez, and D. Mukhedkar, "Analytical modeling of grounding electrodes transient behavior," *IEEE Transactions on Power Apparatus and Systems*, vol. PAS-103, no. 6, pp. 1314–1322, Jun. 1984.

[13] Li, T. Yuan, Q. Yang, W. Sima, C. Sun, and M. Zahn, "Numerical and experimental investigation of grounding electrode impulse-current dispersal regularity considering the transient ionization phenomenon," *IEEE Transactions on Power Delivery*, vol. 26, no. 4, pp. 2647-2658, Oct. 2011.

[14] D. S. Gazzana, A. B. Tronchoni, R. C. Leborgne, A. S. Bretas, D. W. P. Thomas, and C. Christopoulos, "An Improved Soil Ionization Representation to Numerical Simulation of Impulsive Grounding Systems," *IEEE Transactions on Magnetics*, vol. 54, no. 3, pp. 1–4, Mar. 2018.

[15] F. E. Menter, and L. Grcev, "EMTP-based model for grounding system analysis", *IEEE Transactions on Power Delivery*, vol. 9, no. 4, pp. 1838-1849, Oct. 1994.

[16] C. Mazzetti and G. M. Veca, "Impulse Behavior of Ground Electrodes," *IEEE Transactions on Power Apparatus and Systems*, vol. PAS-102, no. 9, pp. 3148-3156, Sept. 1983.

[17] V. Cooray, M. Zitnik, M. Manyahi, R. Montano, M. Rahman and Y. Liu, "Physical model of surge-current characteristics of buried vertical rods in the presence of soil ionization," in *Proc. 2002 International Conference on Lighting Protection*.

[18] M. Mokhtari and G. B. Gharehpetian, "Integration of Energy Balance of Soil Ionization in CIGRE Grounding Electrode Resistance Model," *IEEE Transactions on Electromagnetic Compatibility*, vol. 60, no. 2, pp. 402-413, April 2018.

[19] C. Huygens, Traité de la lumière. 1690.

[20] CIGRE. Guide to procedures for estimating the lightning performance of transmission lines, CIGRE Tech. Brochure 63, Paris, France, 1991.

[21] P. L. Bellaschi, R. E. Armington, and A. E. Snowden, "Impulse and 60–cycle characteristics of driven grounds II," *Transactions of the American Institute of Electrical Engineers*, vol. 61, no. 6, pp. 349–363, 1942.

[22] E.E. Oettle, "The characteristics of electrical breakdown and ionization processes in soil," *The Transactions of the SA Institute of Electrical Engineers*, pp. 63-70, Dec. 1988.